Enhanced Adsorption of Arsenic onto Maghemites Nanoparticles: As(III) as a Probe of the Surface Structure and Heterogeneity

Mélanie Auffan,*[,†,‡] Jérôme Rose,[†,‡] Olivier Proux,[§] Daniel Borschneck,[†,‡] Armand Masion,[†,‡] Perrine Chaurand,[†,‡] Jean-Louis Hazemann,[£] Corinne Chaneac,[||] Jean-Pierre Jolivet,[||] Mark R. Wiesner,[⊥] Alexander Van Geen,[#] and Jean-Yves Bottero[†,‡]

CEREGE, UMR 6635 CNRS-Aix Marseille Université, Europôle de l'Arbois, 13545 Aix-en-Provence, France, IFR PMSE 112, Europôle de l'Arbois, 13545 Aix-en-Provence, France, LGIT, UMR CNRS-Université Joseph Fourier, 1381 rue de la piscine 38400 St Martin d'Hères, France, Institut Néel, 25 avenue des Martyrs, 38042 Grenoble, France, Laboratoire Chimie de la Matière Condensée, UMR 7574 CNRS-UPMC, 75252 Paris, France, Civil and Environmental Engineering, Duke University, Durham, North Carolina 27708-0287, and Lamont Doherty Earth Observatory, Columbia University, Palisades, New York 10964

Received September 28, 2007. In Final Form: December 7, 2007

When normalized per unit of surface area, the quantity of arsenic adsorbed at the maghemite surface remains constant for particles between 300 and 20 nm. However, nanoparticles smaller than 20 nm exhibit enhanced adsorption capacity. The origin of this observed size-dependence for adsorption or "nano effect" is unclear. Arsenic was chosen as a probe of the surface structure to explore adsorption mechanisms occurring at the surface of maghemite nanoparticles (6 nm). Two factors contributing to the enhanced reactivity of nanoscale maghemites were determined. The first is related to a size-dependent structural modification of the surface of particles and the decrease of the occupancy of the tetrahedral site that leaves vacant, highly reactive adsorption sites. In particular, there is a site localized in a six-membered iron octahedral ring. This site is the only one for which an oxidation of As^{III} occurs. The second factor relates to the thermodynamics of a decrease of the surface free energy. The high density of As adsorbed at the saturation of the surface can be related to crystal growth.

Introduction

Nanomaterials and the nanotechnologies they inspire present potential new solutions to major environmental issues,[1,2] as well as uncertainties surrounding impacts of these materials on the environment and human health.[3−6] These opportunities and uncertainties are derived from intriguing differences between the behavior of materials when they are present in bulk and when they are present as nanoscale objects. Nanoparticles are often characterized by a greater reactivity due to their elevated surface/volume ratio. For example, 40% or more of the atoms making up a nanoparticle are present on the surface of particles smaller than 20 nm in diameter.[7] A true nanoscale effect may also be anticipated as distances between functional groups and facets on nanoparticle surface decrease and quantum effects become important. To date, such nanoscale effects have not been elucidated for the case of metal adsorption or complexation as a function of nanoparticle size. Such differences in reactivity might be exploited to improve surface-based reactions in engineered systems as water treatment and soil remediation. Removal of arsenic from water is one such example and the quantity of arsenic adsorbed per gram of magnetite (Fe_3O_4) has been observed to increase from 0.02 to 1.8 mmol/g as particles size decreases from 300 to 11 nm.[8] Much of this 100-fold increase of adsorption capacity for the smaller magnetite particles can be attributed to the increase of specific surface area (SSA) with decreasing size of the particles. However, the comparison of adsorbed quantity per mass of adsorbent reveals nothing about the chemical reactivity and a true "nanoscale effect". When expressed per unit of surface area, magnetite particles of 300 and 20 nm are observed to adsorb similar amounts of As (i.e., ∼6 μmol/m^2 = 3.5 As/nm^2) suggesting similar adsorption mechanisms. Surprisingly, for particles smaller than 20 nm, the adsorption capacity increases and magnetite of 11 nm in diameter adsorbs 3 times more As per square nanometer (∼18 μmol/m^2= 10.9 As/nm^2) than does 20 nm-diameter magnetite (Table 1).[8]

These observations lead to two key questions: (i) why is there a change in adsorption behavior for very small nanoparticles and (ii) is this change linked to modifications of the surface structure? To answer these questions, the adsorption mechanisms at the

* To whom correspondence should be addressed. E-mail: auffan@cerege.fr.

† CNRS/Aix Marseille Université.

‡ IFR PMSE.

§ CNRS/Université Joseph Fourier.

£ Institut Néel.

|| CNRS/UPMC.

⊥ Duke University.

Columbia University.

(1) Bottero, J. Y.; Rose, J.; Wiesner, M. R. Nanotechnologies: tools for sustainability in a new wave of water treatment processes. *Integr. Environ. Assess. Manage.* **2006**, *2* (4), 391−395.

(2) Zhang, W. X. Nanoscale Iron Particles for Environmental Remediation: An Overview. *J. Nanopart. Res.* **2003**, *V5* (3), 323.

(3) Brayner, R.; Ferrari-Iliou, R.; Brivois, N.; Djediat, S.; Benedetti, M. F.; Fievet, F. Toxicological Impact Studies Based on Escherichia coli Bacteria in Ultrafine ZnO Nanoparticles Colloidal Medium. *Nano Lett.* **2006**, *6* (4), 866−870.

(4) Maynard, A. D.; Aitken, R. J.; Butz, T.; Colvin, V.; Donaldson, K.; Oberdörster, G.; Philbert, M. A.; Ryan, J.; Seaton, A.; Stone, V.; Tinkle, S. S.; Tran, L.; Walker, N. J.; Warheit, D. B. Safe handling of nanotechnology. *Nature* **2006**, *444* (16), 267−269.

(5) Wiesner, M. R.; Lowry, G. V.; Alvarez, P. J. J. Assessing the risks of manufactured nanomaterials. *Environ. Sci. Technol.* **2006**, *40* (14), 4337−4445.

(6) Xia, T.; Kovochich, M.; Brant, J.; Hotze, M.; Sempf, J.; Oberley, T.; Sioutas, C.; Yeh, J. I.; Wiesner, M. R.; Nel, A. E. Comparison of the Abilities of Ambient and Manufactured Nanoparticles To Induce Cellular Toxicity According to an Oxidative Stress Paradigm. *Nano Lett.* **2006**, *6* (8), 1794−1807.

(7) Banfield, J. F.; Navrotsky, A. *Nanoparticles and the environment. Reviews in mineralogy and geochemistry*; Mineralogical Society of America: Washington DC, 2001; Vol. 67, p 1753.

(8) Yean, S.; Cong, L.; Yavuz, C. T.; Mayo, J. T.; Yu, W. W.; Kan, A. T.; Colvin, V. L.; Tomson, M. B. Effect of magnetic particle size on adsorption and desorption of arsenite and arsenate. *J. Mater. Res* **2005**, *20*, 3255−3264.

10.1021/la702998x CCC: $40.75
Published on Web 02/12/2008

Table 1. Comparison between the As^{III} Adsorption Efficiency of *Nmag* Obtained in This Study Using ICP-AES with That of Previously Reported Data[a]

			C_{ads} max		
mineral	size (nm)	SSA (m^2/g)	mmol/g	μmol/m^2	arsenic/nm^2
Nmag (this study)	6	174	2.3 ± 0.2	13.4 ± 1.3	8.1 ± 0.8
magnetite[8,25]	~1000	0.9	0.003 ± 0.0003	3.1 ± 0.3	1.9 ± 0.2
	300	4	0.02 ± 0.002	5.6 ± 0.6	3.4 ± 0.3
	20	60	0.39 ± 0.04	6.4 ± 0.6	3.9 ± 0.4
	11	99	1.80 ± 0.2	18.2 ± 1.8	10.9 ± 1.1
hydrous ferric oxide[26]		200	0.37 ± 0.04	1.8 ± 0.2	1.1 ± 0.1
		600	1.34 ± 0.1	2.2 ± 0.2	1.3 ± 0.1
goethite[25,27]		2	0.005 ± 0.0005	2.5 ± 0.3	1.5 ± 0.1
		39	0.29 ± 0.3	7.5 ± 0.8	4.5 ± 0.5

[a] Legend: SSA, specific surface area; C_{ads} max, maximum concentration of As adsorbed at the surface of iron (oxy)hydroxide particles

surface of nanoparticles below 10 nm must be rigorously characterized, studying the adsorption sites and the surface structure from the macroscopic to the atomic scale. The current study focuses on arsenic adsorption processes at the surface of one type of manufactured nanospheres that is widely used and studied—nanomaghemite (γ-Fe_2O_3, referred to as ***Nmag***) with a mean diameter of 6 nm.[9−11] Stimulated by the high affinity of arsenic for iron (hydr)oxides and the worldwide problem of arsenic in drinking water,[12,13] arsenic was chosen as a probe for surface adsorption mechanisms. ***Nmag*** was selected as the adsorbent for this study because these particles have the advantage of being composed of only Fe^{3+} and are stable under ambient conditions. Moreover, they are isotropic and well crystallized and their highly symmetric spinel structure facilitates the examination of surface structure during the adsorption processes. To precisely determine the arsenic adsorption mechanisms at different scales, a panel of techniques of structural characterization was used such as X-ray diffraction, infrared spectroscopy, and X-ray absorption spectroscopy.

Experimental Section

Maghemite Nanoparticles. The 6 nm ***Nmag*** were synthesized at Paris VI university (LCMC) by coprecipitation of Fe^{3+} and Fe^{2+} ions.[11] At the stoechiometry $Fe^{2+}/Fe^{3+} = 0.5$ crystallization of magnetite (Fe_3O_4) with an inverse spinel phase is quasi-immediate at room temperature. Then, because of their high instability against oxidation, the magnetite nanoparticles are transformed into maghemite (γFe_2O_3) by desorption of Fe^{2+} ions and creation of vacancies. Iron atoms are distributed into the tetrahedral (Td = A site) and octahedral (Oh = B site) sites according to ($[Fe^{3+}]_A[Fe_{5/3}{}^{3+}V_{1/3}]_BO_4$) where V stands for vacancies in the octahedral sublattice (Figure 1).[11] On the basis of a 6 nm diameter and a pseudo-spherical shape, the theoretical specific surface area (SSA) of this material is calculated to be 204 m^2/g. This is in reasonable agreement with the measured value of 172 m^2/g determined by N_2 adsorption and a BET analysis where the difference between calculated and measured values is attributed to heterogeneity and partial aggregation of ***Nmag*** during the N_2 adsorption experiment (especially at pH close to the ZPC).

Sorption Experiments. Adsorption studies were performed by mixing 30 mg/L ***Nmag*** with different amounts of 0.013 mol/L $NaAsO_2$ solution in 20 mL flasks. All samples were prepared in 0.01 mol/L NaCl solution at room temperature (22−25 °C), and throughout the experiment, the pH was adjusted at 7 ± 0.2 using standard acid (0.1 mol/L HCl) and base (0.1 mol/L NaOH) solutions. Sorption isotherm was obtained by varying the initial As concentration from 0.1 to 6.5 mmol/L. After 24 h at pH 7 ± 0.2, ***Nmag*** were aggregated since their PZC is around 6.1 and 7.6[14,15] and can be removed from solution by centrifugation during 2 h at 10000 rpm. Arsenic concentrations in the supernatant were measured by ICP-AES (inductively coupled plasma atomic emission spectroscopy) using a Jobin Ultima-C spectrometer.

Triplicate samples with surface coverages of 5%, 10%, and 100% of the maximum adsorption capacity, referred to as, respectively, ***Nmag***As5, ***Nmag***As10, and ***Nmag***As100, were prepared. After the adsorption process the solid phase was rinsed, freeze-dried, and analyzed with the techniques described further.

Powder X-ray Diffraction. X-ray diffraction (XRD) experiments were done on powder samples prepared on a "zero-background" silicon plate and analyzed using a PANalytical X'Pert PRO diffractometer with a Co Kα radiation (1.79 Å) at 40 kV and 40 mA. The 2θ range was 15−120° with a step size of 0.05° with a RTMS (real time multiple strip) detector speed of 0.027°/min leading to a total counting time of 65 h per spectrum. NaCl was used as internal standard to correct a potential shift in the peak positions. The crystalline structure and the structural evolution of ***Nmag*** during the adsorption processes was investigated using a Rietveld refinement.[16] This theoretical calculation was performed using the Fullprof software.[17]

X-ray Absorption Experiments. Arsenic K-edge (11.73 KeV) XAS experiments were performed at the European Synchrotron Radiation Facility (ESRF, France) on the FAME beamline (BM-30b) with Si(220) monochromator crystals.[18,19] By combining the high brilliance from the ESRF synchrotron source with a multichannel fluorescence detector, we were able to obtain spectra with a very high signal/noise ratio even at low As concentration. Samples were

(9) Jolivet, J. P.; Chaneac, C.; Tronc, E. ron oxide chemistry. From molecular clusters to extended solid networks. *Chem. Commun.* **2004**, *5*, 481−487.

(10) Turro, N. J.; Lakshminarasimhan, P. H.; Jockusch, S.; O'Brien, S. P.; Grancharov, S. G.; Redl, F. X. Spectroscopic Probe of the Surface of Iron Oxide Nanocrystals. *Nano Lett.* **2002**, *2* (4), 325−328.

(11) Tronc, E.; Ezzir, A.; Cherkaoui, R.; Chaneac, C.; Nogues, M.; Kachkachi, H.; Fiorani, D.; Testa, A. M.; Greneche, J. M.; Jolivet, J. P. Surface-related properties of γFe2O3 nanoparticles. *J. Magn. Magn. Mater.* **2000**, *221* (1−2), 63−79.

(12) Casiot, C.; Lebrun, S.; Morin, G.; Bruneel, O.; Personne, J. C.; Elbaz-Poulichet, F. Sorption and redox processes controlling arsenic fate and transport in a stream impacted by acid mine drainage. *Sci. Total Environ.* **2005**, *347* (1−3), 122.

(13) VanGeen, A.; Protus, T.; Cheng, Z.; Horneman, A.; Seddique, A. A.; Ahmed, K. M. Testing Groundwater for Arsenic in Bangladesh before Installing a Well. *Environ. Sci. Technol.* **2004**, *38* (24), 6783−6789.

(14) Garcell, L.; Morales, M. P.; Andres-Verges, M.; Tartaj, P.; Serna, C. J. Interfacial and Rheological Characteristics of Maghemite Aqueous Suspensions. *J. Colloid Interface Sci.* **1998**, *205* (2), 470.

(15) Jarlbring, M.; Gunneriusson, L.; Hussmann, B.; Forsling, W. Surface complex characteristics of synthetic maghemite and hematite in aqueous suspensions. *J. Colloid Interface Sci.* **2005**, *285* (1), 212.

(16) Roddick-Lanzilotta, A. J.; McQuillan, A. J.; Craw, D. Infrared spectroscopic characterisation of arsenate(V) ion adsorption from mine waters, Macraes mine, New Zealand. *Appl. Geochem.* **2002**, *17* (4), 445.

(17) Rodriguez-Carvajal, J. Fullprof suite program. 2005, Laboratoire Léon Brillouin.

(18) Proux, O.; Biquard, X.; Lahera, E.; Menthonnex, J.-J.; Prat, A.; Ulrich, O.; Soldo, Y.; 'Evisson, P.; Kapoujyan, G.; Perroux, G.; Taunier, P.; Grand, D.; Jeantet, P.; Deleglise, M.; Roux, J.-P.; Hazemann, J.-L. FAME: A New Beamline for X-Ray Absorption Investigations of Very-Diluted Systems of Environmental, Material and Biological Interests. *Phys. Scr.* **2005**, *T115*, 970−973.

(19) Proux, O.; Nassif, V.; Prat, A.; Ulrich, O.; Lahera, E.; Biquard, X.; Menthonnex, J.-J.; Hazemann, J.-L. Feedback system of a liquid-nitrogen-cooled double-crystal monochromator: design and performances. *J. Synchrotron Radiat.* **2006**, *13*, 59−68.

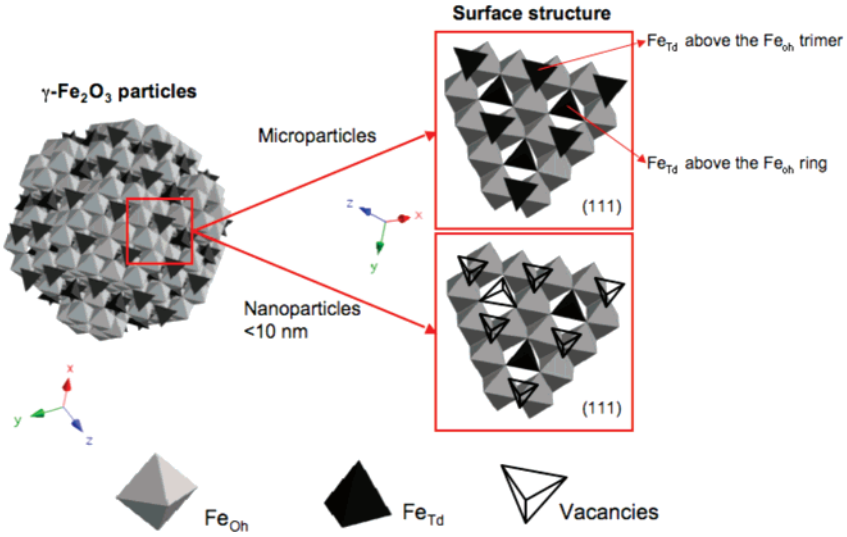

Figure 1. Scheme representing the crystalline structure of maghemite (γ-Fe_2O_3) and the atomic arrangement of the iron tetrahedral (Fe_{Td}) and octahedral (Fe_{Oh}) at the surface (plane (111)) as a function of the size of the particles (based on the study of Brice-Profeta et al.).[24]

pressed to thin pellets, which were cooled to a temperature close to that of liquid Helium (around 10 K) during spectra acquisition. This procedure improves spectrum quality by minimizing radiation damages, decreasing thermal motions of atoms, and keeping As in the same oxidation state during the experiment.[20] XAS spectra were scanned using a step-by-step mode from 100 below to 800 eV above the edge. Multiple scans (3−4) were collected for each sample. To ensure that the high photon flux of the monochromatic beam on FAME beamline did not induce changes in the redox state of As, prior XAS spectra were also acquired in the continuous "quick XAS" scanning mode.[18,19] XANES (X-ray absorption near edge structure) and EXAFS (extended X-ray absorption fine structure) were analyzed using standard procedures for data reduction with a set of software developed by Michalowicz.[21−23] EXAFS oscillations were theoretically recalculated using amplitude and phase functions obtained with the FEFF8 code.[21−23] FEFF functions were validated for each scattering path by modeling the spectra of well-characterized crystalline model compounds (As_2O_3, $FeAsO_4{\cdot}7H_2O$). FEFF8 was also used to estimate the contribution of multiple scattering paths on the EXAFS signal.

Results and Discussion

Adsorption of As^{III} onto *Nmag*. The adsorption isotherm of As^{III} onto ***Nmag*** is shown in Figure 2 plotting the moles of arsenic per square nanometer versus arsenic equilibrium concentration. An experimental maximum is reached at $C_{ads} = 13.4 \pm 0.1$ μmol/m^2 $\approx 8 \pm 0.5$ As^{III}/nm^2 (Figure 2). The measured adsorption capacity of ***Nmag*** for As^{III} is comparable to that reported in literature for magnetite with a size of 11 nm (Table 1).

As^{III} Adsorption Sites as Function of the Surface Coverage. The analysis of samples at low (***Nmag***As5 and ***Nmag***As10) and high (***Nmag***As100) surface coverage is crucial since (i) at low surface coverage arsenite was hypothesized to adsorbed first on the more reactive sites and (ii) at high surface coverage it becomes possible to assess the frequency of the various adsorption surface sites.

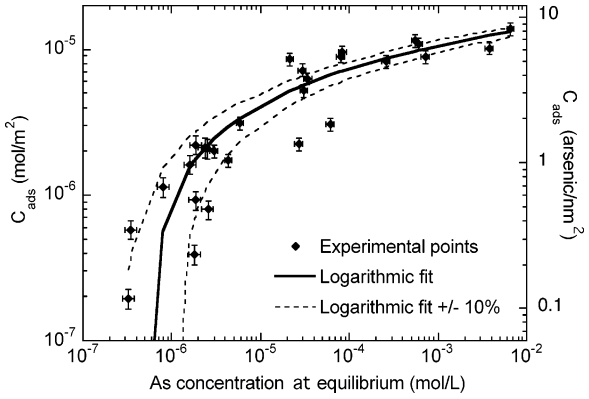

Figure 2. Adsorption isotherm of As^{III} onto ***Nmag***. C_{ads}, concentration of As adsorbed at the ***Nmag*** surface. Dark curve, logarithmic fit. pH 7 ± 0.2, 0.01 M NaCl, [Nm] = 30 mg/L, 22−25 °C.

The consequences of the adsorption of As^{III} onto the ***Nmag*** structure were first studied by X-ray diffraction. The diffraction patterns of the ***Nmag***, ***Nmag***As5, ***Nmag***As10, and ***Nmag***As100 are given in Figure 3A. The position of the main peaks are perfectly superimposed, indicating that structure and crystallinity of the ***Nmag*** are not affected by As adsorption. However the relative intensity of some peaks is modified after As adsorption. The most sensitive is the peak at 21.4° corresponding to the {111} lattice plane (d-spacing = 4.815 Å) for which the normalized intensity decreases when the adsorbed As quantity increases (inset in Figure 3A). The intensity of this peak is highly sensitive to the level of occupancy (σ_A) of the tetrahedral A site of maghemite as illustrated by theoretical calculations (Figure 3B). The sensitivity of the {111} peak to σ_A is related to the fact that the A-oxygen bonds are oriented in the {111} direction. Brice-Profeta et al.[24] have shown that σ_A decreases as the size of maghemite

(20) Meitzner, G.; Gardea-Torresdey, J.; Parsons, J.; Scott, S. L.; Deguns, E. W. The effect of cryogenic sample cooling on X-ray absorption spectra. *Microch. J.* **2005**, *81* (1), 61.
(21) Ankudinov, A. L.; Ravel, B.; Rehr, J. J.; Conradson, S. D. Real space multiple scattering calculation and interpretation of X-ray absorption near-edge structure. *Phys. Rev. B* **1998**, *58* (12), 7565−7576.
(22) Michalowicz, A. EXAFS pour le MAC. *Logiciels Chim.* **1991**, 102−103.
(23) Michalowicz, A. Exafs pour le MAC: a new version of an EXAFS data analysis code for the Macintosh. *J. Phys.* **1997**, *IV* (C2), 235.
(24) Brice-Profeta, S.; Arrio, M. A.; Tronc, E.; Menguy, N.; Letard, I.; Cartier, dit Moulin, C.; Nogues, M.; Chaneac, C.; Jolivet, J. P.; Sainctavit, P. Magnetic order in γ-Fe2O3 nanoparticles: a XMCD study. *J. Magn. Magn. Mater.* **2005**, *288*, 354.
(25) Gimenez, J.; Martinez, M.; de Pablo, J.; Rovira, M.; Duro, L. Arsenic sorption onto natural hematite, magnetite, and goethite. *J. Hazard. Mater.* **2007**, *141* (3), 575−580.
(26) Wilkie, J. A.; Hering, J. G. Adsorption of arsenic onto hydrous ferric oxide: effects of adsorbate/adsorbent ratios and co-occurring solutes. *Colloids Surf. A* **1996**, *107*, 97.
(27) Lenoble, V.; Bouras, O.; Deluchat, V.; Serpaud, B.; Bollinger, J.-C. Arsenic Adsorption onto Pillared Clays and Iron Oxides. *J. Colloid Interface Sci.* **2002**, *255* (1), 52.

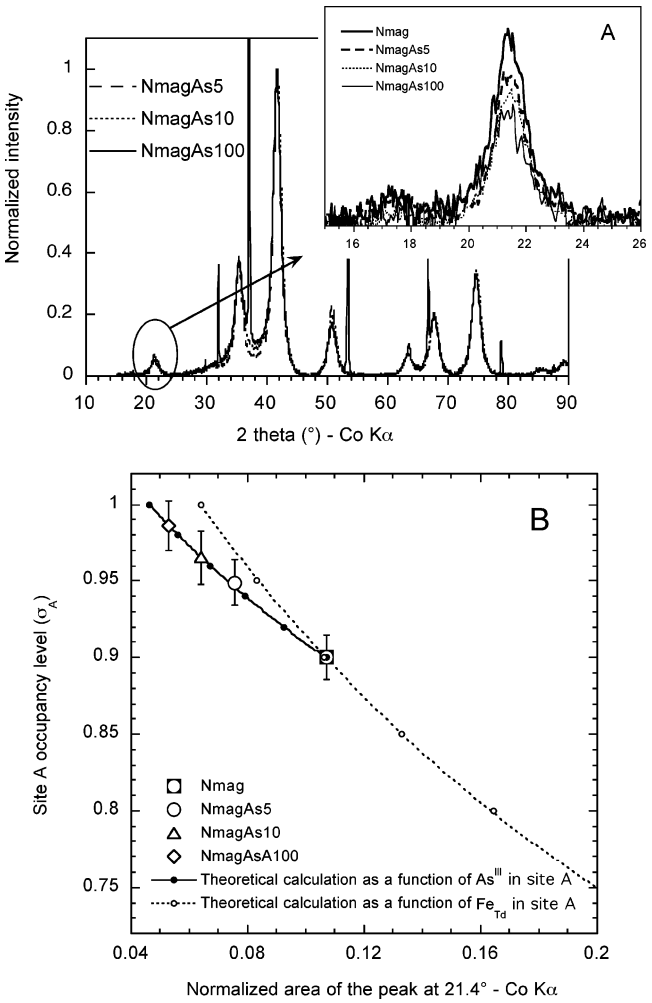

Figure 3. (A) X-ray diffraction patterns of ***Nmag*** as a function of As surface coverage. (B) Theoretical evolution of XRD {111} normalized peak area of standard maghemite as a function of the level of occupancy of the tetrahedral A site with [Fe_{Td}] (dotted line) or As (solid line), compare with experimental values.

particles decreases (Figure 1). They also prove the existence of a preferential iron octahedral layer at the ***Nmag*** surface, which consequently indicates a deficit of [Fe_{Td}] in the A sites at the surface of very small nanoparticles (Figure 1).

On the basis of these results, we performed a first theoretical calculation on the XRD patterns of a standard maghemite (Figure 3B, dotted line). In this calculation, the intensity of the peak {111} was plotted as a function of the level of occupancy of [Fe_{Td}] atoms in the tetrahedral site. Hence, the σ_A for ***Nmag*** before arsenic adsorption was recalculated and we estimate that 90% ± 2% of the A sites are occupied in ***Nmag*** leaving ~10% of the sites A vacant. We assumed that these vacant tetrahedral sites are mainly located in the surface layer of ***Nmag*** as suggested by Brice-Profeta et al.[24] Consequently, by taking into account the volume ($V = 113$ nm^3), the surface ($S = 113$ nm^2) of ***Nmag***, the volume of the maghemite unit cell ($a^3 = 0.581$ nm^3) and the number of tetrahedral sites per unit cell ($N = 8$), an estimate of 1.4 vacant A sites/nm^2 at the surface of ***Nmag*** is obtained using the following equation:

$$\text{surface vacant A sites per nm}^2 = \frac{VN(1-\sigma_A)}{Sa^3} \qquad (1)$$

The decrease of the intensity of the {111} peak observed with the increase of As^{III} surface coverage is attributed to the filling of the surface vacant A sites by As^{III}. As^{III} may be adsorbed in a maghemite lattice position due to the strong affinity to iron oxides, the equal charge to Fe^{III}, and the fact that the O−O−O angles and O−O distances for the AsO_3 molecule are isomorphic to the O−O−O faces of the Fe tetrahedron FeO_4. To confirm this hypothesis, a second theoretical calculation was performed on the XRD pattern of a standard maghemite (Figure 3B, continuous line). In this calculation, the intensity of the peak {111} was plotted as a function of the level of occupancy of As atoms in the tetrahedral lattice position. Hence, the σ_A for ***Nmag***As5, ***Nmag***As10, and ***Nmag***As100 were recalculated as a function of the filling of the 10% of vacant A sites of ***Nmag*** with arsenic. By doing so, the σ_A for ***Nmag***As5 and ***Nmag***As10 was estimated at 94.5% ± 1.5% and 96.5% ± 1.5%, respectively. This suggests (eq 1) that 0.8 ± 0.25 (for ***Nmag***As5) and 0.5 ± 0.25 A sites/nm^2 (for ***Nmag***As10) remain vacant. Since the maximum surface vacancy for A sites was estimated to be 1.4 per nm^2, we deduce that there are 0.6 ± 0.3 A sites/nm^2 for ***Nmag***As5 and 0.9 ± 0.3 A sites/nm^2 for ***Nmag***As10 occupied by As^{III}. Since for ***Nmag***As10 only 0.7 ± 0.07 As/nm^2 are adsorbed, the vacant A structural sites appear to have unique characteristics. Since As replaces [Fe_{Td}] in the A site, this implies that As is bound to a high number of iron octahedra from the B sites; 5 at a theoretical maximum. EXAFS results discussed below confirm this hypothesis. For ***Nmag***As100, the σ_A was estimated at 99% ± 2%, suggesting that all the A sites are occupied by arsenic. Since almost 8 As/nm^2 are adsorbed and the vacant structural A sites can only accommodate 1.4 ± 0.3 As/nm^2, this implies that at least one other type of As surface site must exist.

X-ray absorption spectroscopy at the As K-edge (11.73 KeV) was used to characterize these adsorption surface sites at the atomic scale. EXAFS spectra allow for a precise determination of the local order around the central As absorbing atoms. Previous work using EXAFS spectroscopy has investigated the adsorption of As^{III} on iron (oxy)hydroxide larger than 20 nm. Evidence of three types of complexes has been obtained—a binuclear bridging complex ($R_{AsIII-FeIII}$ = 3.30−3.38 Å), a linear monodentate complex ($R_{AsIII-FeIII}$ = 3.57−3.60 Å), and an edge-sharing complex ($R_{AsIII-FeIII}$ = 2.80−2.81 Å).[28−35] XANES spectra were carefully analyzed to obtain information on the valence state of the arsenic.

In the "quick XAS" configuration, XANES acquisition was performed within 40 s in order to follow a possible change in shape under the X-ray beam. These spectra revealed two

(28) Manceau, A. The mechanism of anion adsorption on iron oxides: Evidence for the bonding of arsenate tetrahedra on free Fe(O, OH)6 edges. *Geochim. Cosmochim. Acta* **1995**, *59* (17), 3647.

(29) Manning, B. A.; Fendorf, S. E.; Goldberg, S. Surface Structures and Stability of Arsenic(III) on Goethite: Spectroscopic Evidence for Inner-Sphere Complexes. *Environ. Sci. Technol.* **1998**, *32* (16), 2383.

(30) Sherman, D. M.; Randall, S. R. Surface complexation of arsenic(V) to iron(III) (hydr)oxides: structural mechanism from ab initio molecular geometries and EXAFS spectroscopy. *Geochim. Cosmochim. Acta* **2003**, *67* (22), 4223.

(31) Thoral, S.; Rose, J.; Garnier, J. M.; vanGeen, A.; Refait, P.; Traverse, A.; Fonda, E.; Nahon, D.; Bottero, J. Y. XAS Study of Iron and Arsenic Speciation during Fe(II) Oxidation in the Presence of As(III). *Environ. Sci. Technol.* **2005**, *39* (24), 9478.

(32) Waychunas, G. A.; Davis, J. A.; Fuller, C. C. Geometry of sorbed arsenate on ferrihydrite and crystalline FeOOH: Re-evaluation of EXAFS results and topological factors in predicting sorbate geometry, and evidence for monodentate complexes. *Geochim. Cosmochim. Acta* **1995**, *59* (17), 3655.

(33) Waychunas, G. A.; Rea, B. A.; Fuller, C. C.; Davis, J. A. Surface chemistry of ferrihydrite: Part 1. EXAFS studies of the geometry of coprecipitated and adsorbed arsenate. *Geochim. Cosmochim. Acta* **1993**, *57* (10), 2251.

(34) Manning, B. A.; Hunt, M. L.; Amrhein, C.; Yarmoff, J. A. Arsenic(III) and Arsenic(V) Reactions with Zerovalent Iron Corrosion Products. *Environ. Sci. Technol.* **2002**, *36* (24), 5455−5461.

(35) Zhang, N.; Blowers, P.; Farrell, J. Evaluation of Density Functional Theory Methods for Studying Chemisorption of Arsenite on Ferric Hydroxides. *Environ. Sci. Technol.* **2005**, *39* (13), 4816−4822.

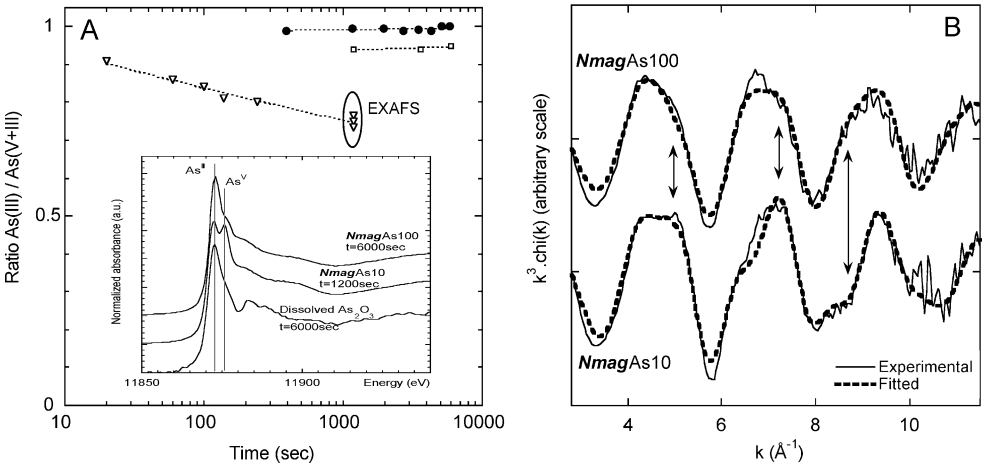

Figure 4. (A) As^{III}/As^{III+V} ratio in function of the exposition time under X-ray beam obtained by linear combination of XANES spectra of As_2O_3 and As_2O_5. Dotted lines, linear fitting; ●, dissolved As_2O_3; ▽, ***Nmag***As10, □: ***Nmag***As100. (B) EXAFS spectra (As K-edge) of ***Nmag***As10 and ***Nmag***As100, experimental data (solid line) and simulation (dotted line).

Table 2. Structural Parameters Deduced from the EXAFS Analysis at the As K-Edge[a]

sample	atomic shell	*N* ±20%	*R* (Å) ±0.02 Å	σ (Å) ±0.01 Å
NmagAs10	As−O	3.6	1.72	0.071
	As−O−O^{MS}	5.0	3.08	0.100
	As−Fe*	3.1	3.41	0.108
NmagAs100	As−O	3.2	1.76	0.061
	As−Fe*	1.7	3.33	0.102

[a] Legend: N, coordination number; *R*, interactomic distance; σ, Debye−Waller factor; As−O−O^{MS}, multiple scattering of the photoelectron; As−Fe shells, iron atoms present in the second coordination sphere of As.

absorption peaks centered on 11873 and 11875 eV characteristic of the As^{III} and As^{V} valence states, respectively (inset in Figure 4A). For each spectrum, we used linear combination of XANES spectra of pure As^{III} and As^{V} samples to determine the $As^{III}/As^{(III+V)}$ ratio evolution with time (Figure 4A). In the initial state, the ratio is close to 1 for both samples, ***Nmag***As10 and ***Nmag***As100. With an increasing counting time under the X-ray beam, two different behaviors are observed—an arsenite oxidation appeared for ***Nmag***As10 with irradiation time (even at 10 K) while the ***Nmag***As100 remained stable over long scanning times. We estimate that 30% of As^{III} of ***Nmag***As10 was oxidized after 15 min under the beam. For ***Nmag***As100, only 7% of the adsorbed As^{III} was oxidized which is in agreement with the fraction of As^{III} oxidized for the ***Nmag***As10 sample. These differences in oxidation under X-ray beam reflect (i) the strong reactivity of As for sites where oxidation takes place and (ii) the presence of very different adsorption sites as already suggested by the adsorption and diffraction experiments.

EXAFS spectra also revealed differences between ***Nmag***As10 and ***Nmag***As100 spectra with different features at 5.2, 7.4, and 8.7 $Å^{-1}$ (Figure 4B). The modeling of these EXAFS spectra allows to quantify these differences and to precise the local structures. The first coordination sphere corresponds to As−O bonds: its length increases from 1.72 to 1.77 ± 0.02 Å while the number of As−O contributions decreased from 3.4 to 3.1 ± 0.6 for ***Nmag***As10 and ***Nmag***As100, respectively (Table 2). It is also necessary to include a multiple scattering contribution of As−O−O to satisfactorily reproduce the experimental spectra of ***Nmag***As10. The bond length values can be directly compared to the ones obtained for reference compounds: the As^{V}−O distances (1.60−1.73 Å range) are generally shorter than the As^{III}−O ones (1.77−1.80 Å range).[36] The EXAFS simulations then appear to confirm the XANES results, i.e., the presence of As^{V} for the ***Nmag***As10 sample.

The second coordination sphere of As corresponds to an As−Fe contribution (Table 2). At low adsorption quantities (***Nmag***As10), this contribution is characterized by 3.1 ± 0.6 iron atoms (N_{Fe}) at 3.40 ± 0.02 Å. The As−Fe distance is very close to the average As^{III}−Fe^{III} interatomic distance of 3.31−3.40 Å attributed to As^{III}−O−Fe linkages through double-corner-sharing in literature.[28−33] However, the high iron coordination number N_{Fe} is not in agreement with a pure double-corner-sharing surface complex since N_{Fe} should be 2 in such a configuration. XRD results have previously highlighted that for this surface coverage, arsenic fills the A surface sites on the {111} lattice plane. By examining the cation in this A site (Figure 5), it appears that the cation is linked via three double corner linkages to five irons at maximum. Consequently, in such an adsorption site, arsenic can be linked with more than two iron atoms with an As−Fe distance characteristic of a double corner linkage. The EXAFS results corroborate this hypothesis. Indeed, the obtained-contribution of 3.1 ± 0.6 Fe atoms at 3.40 ± 0.02 Å of arsenic could be in agreement with As adsorbed in the A vacant site to more than two iron atoms through double corner linkage.

At high surface coverage (***Nmag***As100), the number of Fe atoms obtained by EXAFS in the second coordination sphere of As decreases to 1.7 ± 0.3 and the As−Fe distance is 3.33 ± 0.02 Å (Table 2). This latter observation indicates that at high surface coverage arsenite adsorbed on a second site with lower Fe coordination number. This adsorption site will be discussed below.

In both cases (***Nmag***As10 and ***Nmag***As100), it is important to note that the σ values for the As^{III}−Fe linkages are elevated (between 0.102 and 0.108) (Table 2). Using reference compounds (coprecipitated As^{V}/Fe)[31] and surface χ^2 analysis, we have demonstrated that the *N* and σ values corresponding to the minimum χ^2 ± 10% are in the ranges 3−3.8 and 0.100−0.120, respectively, for ***Nmag***As10. Hence, the high σ values are physically significant and may be due to structural disorder related to the very reactive surface. This indicates that the local atomic environment obtained for As at low (3.1 ± 0.6 Fe neighbors) and high surface coverage (1.7 ± 0.3 Fe neighbors) are not due to mathematic artifact.

(36) Farquhar, M. L.; Charnock, J. M.; Livens, F. R.; Vaughan, D. J. Mechanisms of Arsenic Uptake from Aqueous Solution by Interaction with Goethite, Lepidocrocite, Mackinawite, and Pyrite: An X-ray Absorption Spectroscopy Study. *Environ. Sci. Technol.* **2002**, *36* (8), 1757−1762.

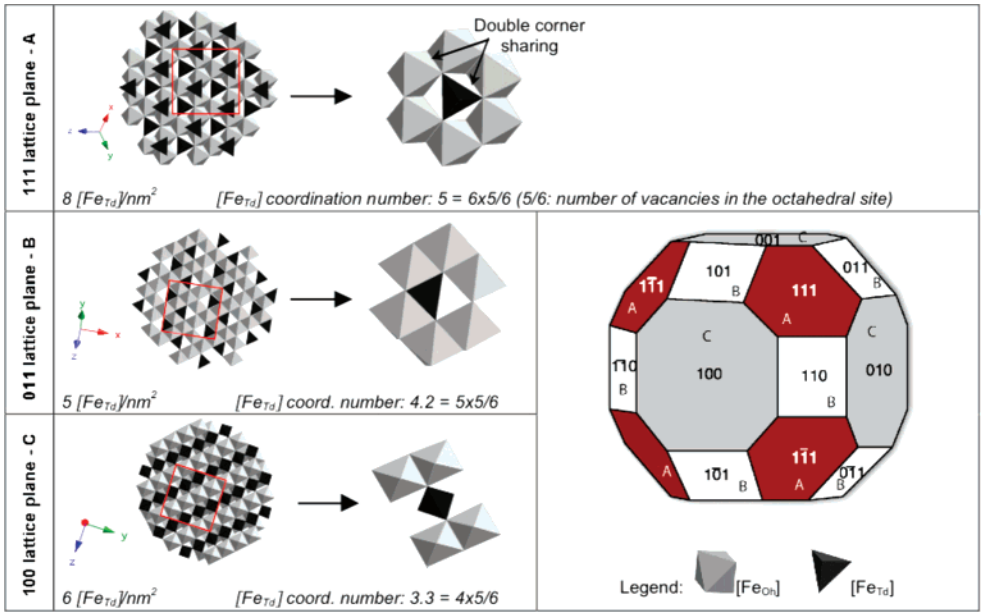

Figure 5. Assumed equilibrium energy shape of the particles (based on a Kossel model) and structure of the three main lattice planes at the surface of ***Nmag***. This figure gives an estimation of the coordination number of [Fe$_{Td}$] in the octahedral ring. Red square: 1 nm^2.

Specificity of the Arsenite Adsorption Mechanisms on Ultrafine Nanomaghemite. Structural information concerning the As surface layer has been obtained from EXAFS results (Figure 4B, Table 2). For ***Nmag***As100 and ***Nmag***As10, the As^{III}−Fe distances of 3.33−3.41 ± 0.02 Å are in agreement with double corner linkage between As^{III} and [Fe$_{Oh}$]. However, if we examine the {111} surface, the possibility of double corner linkage at the ***Nmag*** surface only exists at the edge of the plane, suggesting a low number of possible sites. This statement is not in agreement with the high quantity of As at the plateau (∼8 As/nm^2), indicating that the surface sites are different than those of the 'classical' adsorption sites on a larger iron oxide particles. Moreover, the high surface density of arsenite cannot be attributed to a structural modification of the ***Nmag***, such as amorphization of the surface, the crystallinity of ***Nmag*** being constant as determined by XRD. It therefore seems that some specific As adsorption sites exists at the surface of ***Nmag*** based on the deficiency of [Fe$_{Td}$] at the surface (Figure 1). As previously mentioned, arsenite can be considered as isomorphic to [Fe$_{Td}$] with the same charge and Pauli radius. Hence, As^{III} is physically able to occupy the free [Fe$_{Td}$] lattice positions at the surface of ***Nmag*** (as demonstrated by XRD, Figure 3). These free [Fe$_{Td}$] lattice positions represent a high density of adsorption sites at the surface since the number of tetrahedral sites per square nanometer, reaches 8, 5, and 6 for the {111}, {011}, and {100} surface planes, respectively (Figure 5). This is in agreement with the high quantity of As at the plateau (∼8 As/nm^2). Examination of the {111} plane suggests that the As may be linked (i) 'in' the A vacant site (octahedral ring) surrounded by 5 [Fe$_{Oh}$] sites at maximum through double corner sharing or (ii) 'on' a B trimer through single corner sharing, but linked to no more than 3 [Fe$_{Oh}$] (Figure 1). In both cases, the As^{III}−Fe interatomic distance are in the same range, but to go further, better determinations for the theoretical coordination number of iron around As (N$_{Fe}$) are needed as obtained by EXAFS. Indeed, there is still a discrepancy between the obtained value of 3.1 ± 0.6 for ***Nmag***As10 and 1.7 ± 0.3 for ***Nmag***As100 and the theoretical coordination of cations on the {111} lattice plane: ∼5 in the octahedral ring and ∼3 on the B trimer.

To understand this discrepancy, we assume an equilibrium shape for the 6 nm ***Nmag*** crystals. Brice-Profeta et al. observed that crystallized ***Nmag*** (synthesized in exactly the same manner as our initial material), exhibited well-defined faceted edges but with no shape anisotropy.[24] To approximate the shape of the ***Nmag*** crystals, we use a Kossel model (cubic theoretic crystal). By taking into account the second nearest-neighbors interaction and applying the Wulf theorem, the equilibrium shape of a 2D crystal is calculated to be an octogon and a 26-face polyhedron for the 3D crystal (Figure 5).[37] Three different faces exist on the polyhedron corresponding to the three densest lattice planes {111}, {100}, and {110} of a cubic structure.

To explain the N_{Fe} of 3.1 ± 0.6 obtained for ***Nmag***As10, we determine the coordination number of [Fe$_{Td}$] localized 'in' the A vacant site (octahedral ring) for the three main planes. For {111}, {100}, and {110} the coordination number is estimated at 5, 4.2, and 3.3, respectively (Figure 5). If the three planes are equivalent, then the mean Fe coordination number will be 4.1. By considering that all faces of the polyhedra exhibit the same surface, we estimate the surface area of each face at 4.3 nm^2. Therefore, due to the low extension of the plane and the size of the unit cell (0.837 nm), at least one-third of the A sites of each plane will be at the edge with a coordination number estimated at 2 or 3. Then the mean total coordination number of [Fe$_{Td}$] in the octahedral ring is certainly close to 3.5 ± 0.5. Although this coordination value is based on several simplifying assumptions, it reasonably explains the N_{Fe} value of 3.1 ± 0.6 around As obtained for the ***Nmag***As10. Therefore, we conclude that the adsorption of As^{III} for low adsorption quantities most likely occurs in the octahedral ring 'in' the A vacant site. As determined by XRD, this site adsorbed 0.9 As^{III}/nm^2. Moreover, the X-ray beam damage (Figure 4A) illustrates the high reactivity of this surface site for which the electron transfer between arsenic and the octahedral ring seems to be facilitated (X-ray beam effects).

To explain the value obtained for N_{Fe} of 1.7 ± 0.3 for ***Nmag***As100, we calculate in the same manner the coordination number of [Fe$_{Td}$] localized 'on' the B trimer for the {111}, {100}, and {110} planes to be 2.5, 1.7, and 1.7, respectively (Figure 6). By considering that the three planes are equivalent and that one-third of the A sites are at the edge of the face with a coordination number estimated at 1 or 2, we estimate the mean coordination

(37) Mutaftschiev, B. *The atomistic nature of crystal growth*; Springer-Verlag: Berlin, 2001; Vol. 43, p 368.

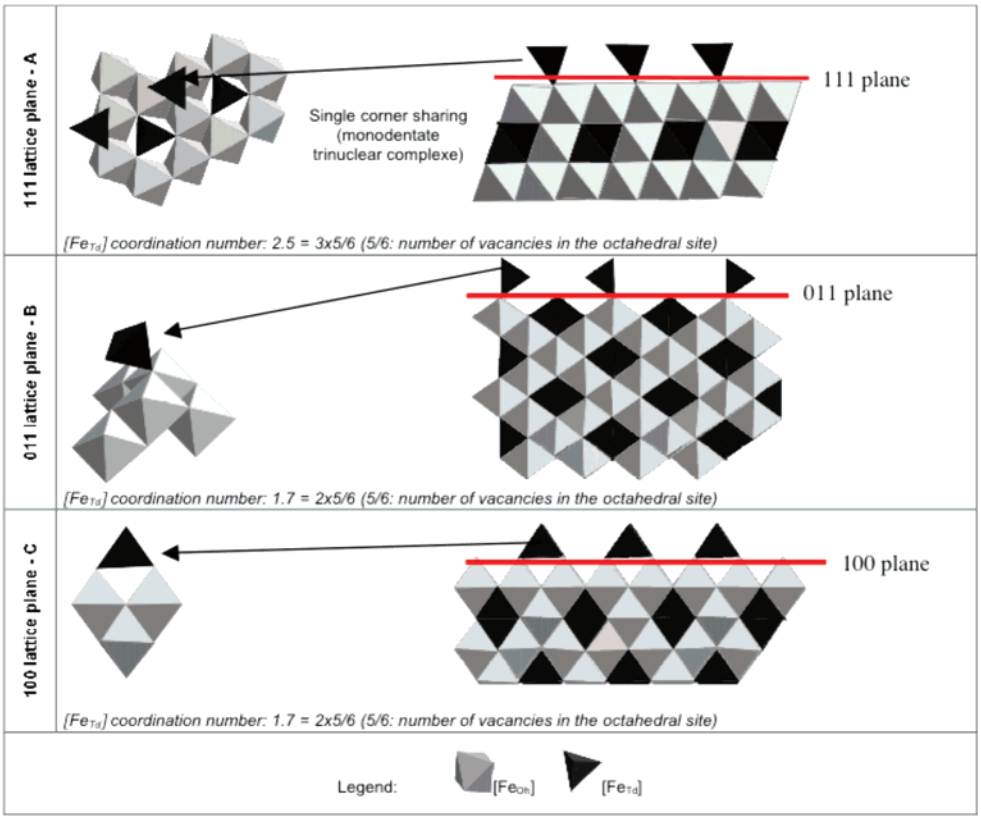

Figure 6. Structure of the three main lattice planes at the surface of ***Nmag***. This figure gives an estimation of the coordination number of [Fe_{Td}] on the B trimer.

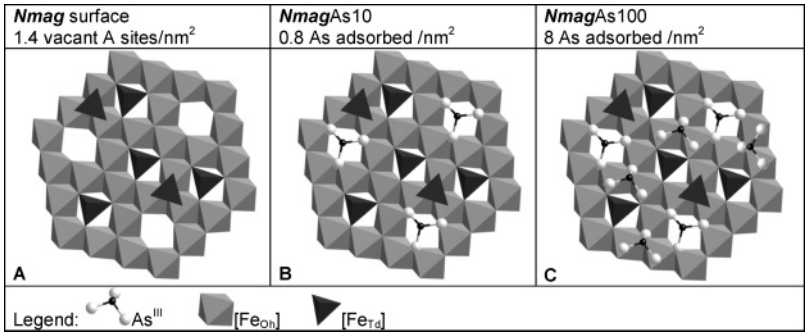

Figure 7. Scheme representing the adsorption mechanisms of As^{III} at the ***Nmag*** surface based on the structural information derived from the XRD and As K-edge XAS analyses.

number of [Fe_{Td}] on the B trimer as to 1.8 ± 0.2. Further, by considering that As localized on the B trimer represents 7.1 of the 8 As^{III} adsorbed per square nanometer (the other 0.9 As^{III}/nm^2 being linked in the A vacant site) we obtain an estimate of 2 ± 0.2 for the mean total Fe coordination number around As on the saturated surface. This value, based on several simplifying assumption, explains reasonably the N_{Fe} value of 1.7 ± 0.3 around As obtained for the ***Nmag***As100.

In summary, different mechanisms of As^{III} adsorption appear to dominate as a function of the surface coverage. Initially, 1.4 tetrahedral sites per square nanometer are vacant at the surface of ***Nmag*** (Figure 7A). At low surface coverage, arsenic fills the more reactive surface sites in the octahedral ring (Figure 7B). When all of these sites are filled, arsenite adsorbs on a [Fe_{Oh}] trimer through monodentate trinulear complex in a lattice position (Figure 7C).

Hence, we can explain the high As density (8 ± 0.5 As^{III}/nm^2) by considering As^{III} adsorbed in the [Fe_{Td}] lattice position. However, why for nanoparticles (<20 nm) the As occupy the lattice position of [Fe_{Td}] whereas for larger particles, As^{III} is classically adsorbed through double- or single-corner-sharing?[38] It is worth noting that nanoparticles are thermodynamically unstable compared with microscopic particles. Many phenomena may intervene in producing a decrease in the surface free energy, including changes in surface site coordination, displacement of atoms, change in bond length and angles and, aggregation or adsorption of chemical species.[7] Adsorption of ions at the surface of particles decreases the energy (ΔG) of a system by $\Delta G = 3.V_m\Delta\gamma/r$, where V_m is the molar volume, $\Delta\gamma$ is the difference of the interfacial energy before and after adsorption and r is the radius of the particles. Using the method presented by Jolivet et al.[39] we estimate that as a consequence of the adsorption of one monolayer of arsenic at the surface of iron oxide particles of 6,

(38) Coker, V. S.; Gault, A. G.; Pearce, C. I.; Vanderlaan, G.; Telling, N. D.; Charnock, J. M.; Polya, D. A.; Lloyd, J. R. XAS and XMCD Evidence for Species-Dependent Partitioning of Arsenic During Microbial Reduction of Ferrihydrite to Magnetite. *Environ. Sci. Technol.* **2006**, *40*, 7745−7750.

(39) Jolivet, J. P.; Froidefond, C.; Pottier, A.; Chanéac, C.; Cassaignon, S.; Tronc, E.; Euzen, P. Size tailoring of oxide nanoparticles by precipitation in aqueous medium. A semi-quantitative modelling *J. Mater. Chem.* **2004**, *14*, 3281−3288.

20, and 300 nm, the $\Delta\gamma$ decreases by 0.2−0.3 J/m^2 (∼3 kT), 0.002−0.003 J/m^2 and 0.0005, respectively. Comparing the different systems characterized by $r_{6nm}\langle r_{20nm}\langle r_{300nm}$ and $\Delta\gamma_{6nm}\rangle\rangle\rangle\Delta\gamma_{20nm}\rangle\Delta\gamma_{300nm}$ we observe that adsorption of a dense arsenite layer on nanoparticles of 6 nm decreases the energy of the system more than adsorption on larger particles of 20 or 300 nm ($\Delta G_{6nm}\rangle\rangle\rangle\Delta G_{20nm}\rangle\Delta G_{300nm}$). Whereas in macroscopic systems the adsorption is mainly governed by the chemical affinity and the electrostatic strength, for nanoparticles, the decrease of free energy must be taken into account. This driving force is known to be preponderant in the case of crystal growth. In our study, the adsorption of As^{III} in the free [Fe$_{Td}$] lattice position at the ***Nmag*** surface can be compare to a crystal growth mechanism in which As^{III} mimics the [Fe$_{Td}$] atoms. This may explain the high density of As adsorbed at the surface of ***Nmag***.

Conclusion

Two factors appear to contribute to an observed "nanoeffect" of enhanced As^{III} adsorption by nanoiron oxides below 20 nm in diameter. First, there is a modification of the atomic structure of the particle surface as size decreases.[24] In the case of ***Nmag***, the size-dependent decrease of the occupancy of the tetrahedral site leaves vacant, highly reactive sites, which are available to adsorb arsenic. For larger particles, the ratio B/A at the surface seems to be closer to the theoretical value[24] with fewer vacant A sites and therefore fewer accessible sites. Moreover, the presence of [Fe$_{Td}$] at the surface prevents the adsorption of arsenite through monodentate trinuclear complexes due to steric constraints. Only double or single corner sharing adsorbing complexes remain probable.[38] The second factor relates to the thermodynamics of a decrease of the surface free energy. The high density of As adsorbed in lattice position at the surface can be related to crystal growth.

Acknowledgment. This program has been funded by the French National Program ACI-FNS (ANR) "ECCO" supported by INSU (French National Institute for Earth Sciences and Astronomy). The XAS work was performed at the European Synchrotron Radiation Facilities, Grenoble, France. We are grateful to the machine and beamline groups whose outstanding efforts have made these experiments possible.

LA702998X